ISSN: 2832-4293

Pan-American Journal of Mathematics 5 (2026), 1
https://doi.org/10.28919/cpr-pajm/5-1

MODELING THE GLUCOSE-INSULIN-GLUCAGON INTERACTIONS

SALMA AL-TUWAIRQI*, KHLOOD ALAMER, AND HUNIDA MALAIKAH

ABSTRACT. This research presents a mathematical model that investigates the regulation of glucose levels in the human body through interactions with insulin and glucagon. The model accounts for the action of incretin hormones in the intestine, which stimulates the release of insulin. The study uniquely combines sensitivity analysis and equilibrium stability analysis to provide a comprehensive understanding of these interactions. A system of nonlinear ordinary differential equations is formulated to describe the model's dynamics. Qualitative analysis ensures the positivity and boundedness of state variables, identifies a unique steady-state solution, and establishes its local and global asymptotic stability. Sensitivity analysis further elucidates the complicated relationships between glucose, insulin, and glucagon, highlighting the impact of key parameters on glucose equilibrium levels. Numerical simulations validate the theoretical findings, demonstrating the model's robustness and reliability. The study's findings have significant implications in the real world, particularly in the advancement of clinical and therapeutic strategies for managing diabetes. By offering insights into the mechanisms of glucose regulation, the model provides a valuable framework for optimizing treatments and developing targeted interventions for metabolic disorders.

1. INTRODUCTION

The human body requires three fundamental types of fuel: glucose, lipids, and proteins to support optimal physiological function. Among these, glucose is the most accessible energy source and plays a crucial role in metabolism and hydration [1]. Maintaining a consistent glucose concentration in the blood plasma, typically between 60 and 100 mg/dL, is vital for normal bodily function [2]. During physical activity or stress, muscles demand a higher concentration of glucose to perform efficiently.

Pancreatic endocrine hormones, including insulin, glucagon, somatostatin, and amylin, primarily regulate blood glucose levels. Insulin, a peptide hormone secreted by pancreatic beta cells, facilitates the uptake of glucose into cells, where it is utilized for energy production. In contrast, glucagon, secreted by pancreatic alpha cells, raises blood glucose levels by promoting glycogenolysis, the breakdown of glycogen into glucose in the liver, and by stimulating gluconeogenesis, the synthesis of glucose from non-carbohydrate sources [3]. This dynamic interplay between insulin and glucagon ensures that cells receive adequate energy while preventing persistent hyperglycemia or hypoglycemia [4].

Numerous studies have investigated the complex relationship between glucose and insulin, and several models have been developed to describe glucose homeostasis. In [5], a delay differential equation model was created to simulate pancreatic insulin secretion in type 1 diabetes patients with elevated glucose concentrations, along with exogenous insulin infusion. The study in [6] examined the impact of diabetes factors

DEPARTMENT OF MATHEMATICS, KING ABDULAZIZ UNIVERSITY, JEDDAH, SAUDI ARABIA
E-mail addresses: saltuwairqi@kau.edu.sa, kalamer0002@stu.kau.edu.sa, hmalaikah@kau.edu.sa.
Submitted on Oct. 05, 2025.
2020 *Mathematics Subject Classification.* 34C60, 34D20, 34D23, 92D30.
Key words and phrases. mathematical model; glucose; insulin; glucagon; stability; sensitivity analysis.
*Corresponding author.

on the onset of the oscillatory regime and presented four strategies for restoring healthy control. Where it was extended in [7] by incorporating a temporal delay in the glucose-insulin interaction term.

Ma and Li in [8] illustrated the interaction between glucose and insulin, aiming to assist patients in reducing pain and achieving optimal hypoglycemic effects. In [9], they developed a simplistic model to predict the role of vitamin D in the glucose-insulin regulation system. The model in [10] was formulated, comprising glucose levels, insulin levels, and beta-cell mass.

A realistic model in [11] was developed by incorporating ingested glucose as a new parameter representing external glucose acquired through food consumption. In [12], a mathematical model of the glucose-insulin regulation system was presented, incorporating ingested glucose as a new variable. The model in [13] incorporated three compartments: plasma glucose, plasma insulin, and interstitial insulin, which represent insulin in non-plasma tissues and are known as the remote insulin compartment.

Lombarte et al. [14] created a mathematical model to investigate glucose and insulin homeostasis in healthy rats. Although this model has only been used on healthy rats, the ultimate goal is to adapt and validate it in both in vivo and in silico models for diabetic animals. A new model, presented in [15], was introduced, which provides a mathematical formulation of the theoretically predicted insulin concentrations, representing insulin secretion from beta-cells after glucose intake. Furthermore, the glucose rate of appearance is derived from glucose absorption along the gastrointestinal tract, represented by a sequence of three comparable models. The model in [16] focused on the dynamic modeling of the glucose-insulin system with pulse injection of insulin analogues and glucosidase inhibitors.

In [17], the model uses a fractional operator to analyze glucose homeostasis, incorporating beta-cells, insulin, glucose, and growth hormone. It provides a comprehensive understanding of glucose-insulin dynamics and offers a framework for diabetes management strategies. Other models that utilize fractional derivatives for glucose-insulin regulation are presented in [18, 19].

Other studies have analyzed models that incorporate the effect of glucagon on glucose regulation dynamics. For example, Uluseker et al. [20] presented a multi-level, closed-loop model of glucose homeostasis, describing the interactions between glucose, hormones, and tissues. They illustrated simulations of normal glucose regulation and conditions associated with type 2 diabetes.

Recently, in [21], a model was developed to understand the paracrine roles of insulin and glucagon in glucose-stimulated hormonal secretion by pancreatic alpha- and beta-cells. This model predicted both transient and steady-state profiles of insulin and glucagon secretion. Moreover, in [22], they analyzed the effect of alpha-and beta-cell dysfunction on type 2 diabetes through a glucose-insulin-glucagon model using isoglycemic intravenous glucose infusion (IIGI) data. They found a strong connection between glucagon suppression and diabetes markers. In [23], they extended a model for type 1 diabetes to integrate glucagon dynamics explicitly. By comparing simulations with the original model, they established that glucagon contributes to the safety of the artificial pancreas.

The complex interactions between glucose, insulin, and glucagon are crucial in regulating blood glucose levels. This study is motivated to capture these interactions and provide a robust analysis of stability and sensitivity. A comprehensive mathematical framework is developed that incorporates, in addition to the three main compartments, two compartments: glucose in the stomach and glucose in the intestine, to account for the release of insulin influenced by incretin hormones in the intestine.

This work is organized as follows. In Section 2, we establish the model and demonstrate its well-posedness. Section 3 provides a qualitative analysis of the model, which includes an examination of equilibrium points along with their local and global stabilities. Additionally, in Section 4, we conduct a numerical analysis to validate the qualitative findings through numerical experiments. This section also includes a

sensitivity analysis of the model's parameters, as well as the sensitivity of the equilibrium point in relation to these parameters.

2. Model Structure

The model comprises five compartments: glucose quantity in the stomach, S; glucose quantity in the intestine, N; plasma glucose concentration, G; insulin concentration, I; and glucagon concentration, C. The state variables, $S,\ N,\ G,\ I$, and C, are functions of the independent variable time, t. The assumptions describing the dynamics of the model's interaction between glucose, insulin, and glucagon are as follows. An initial dose of glucose, D, is administered to the stomach. Then, the glucose within the stomach transfers to the intestine at a rate of α. An initial release of glucose from the intestine to the plasma occurs at a rate of β_1, followed by a later release of glucose to the plasma at a rate of β_2 [24]. When glucose enters the digestive system, it stimulates the release of incretin hormones, promoting insulin secretion at a rate of σ_1. Also, the discharge of glucose into the plasma triggers the pancreas to secrete insulin into the plasma at a rate of σ_2. Some cells, such as brain cells, uptake glucose independently of insulin at a rate of μ_2, while others depend on insulin for uptake at a rate of μ_1. As blood glucose levels decline, in the case of glycemia, the pancreas activates α cells to secrete glucagon at a rate of σ_3. Glucagon stimulates gluconeogenesis in the liver, releasing glucose into the bloodstream at a rate of P [25].

Glucagon in the blood is associated with lower insulin levels; likewise, high insulin levels reduce glucagon levels. We assume that the decay rates of insulin due to glucagon concentration and that of glucagon due to insulin concentration are d_3 and d_4, respectively. Moreover, the kidneys and liver are responsible for the primary breakdown of insulin and glucagon [26]; therefore, we consider the clearance rates of insulin and glucagon to be d_1 and d_2, respectively.

The following nonlinear system of ordinary differential equations governs the dynamics of the model:

$$\begin{aligned} S' &= -\alpha S,\ S(0) = D, \\ N' &= \alpha S - (\beta_1 + \beta_2)N, \\ G' &= (\beta_1 + \beta_2)N - \mu_1 GI - \mu_2 G + PC, \\ I' &= \sigma_1 N + \sigma_2 G - d_1 I - d_3 C, \\ C' &= \sigma_3 G - d_2 C - d_4 I. \end{aligned} \tag{2.1}$$

All the parameters in the model are positive. Table 1 briefly summarizes the model's parameters. Additionally, Figure 1 presents a block diagram of the model, providing a schematic representation of the compartments and their interactions.

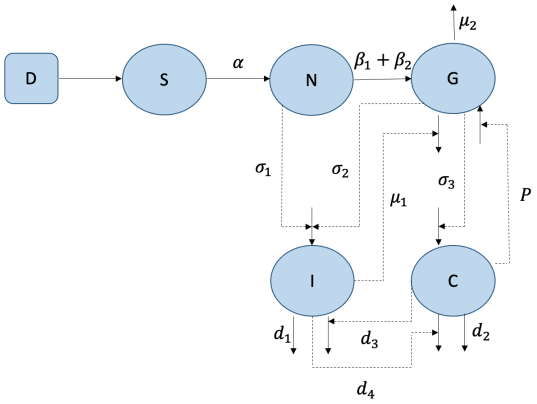

Figure 1. Flowchart of model (2.1).

TABLE 1. Description of models' parameters.

Parameter	Description
α	Glucose transfer rate from stomach to intestine
β_1	Glucose transfer rate from jejunum to plasma
β_2	Glucose transfer rate from ileum to plasma
μ_1	Insulin-dependent glucose elimination rate
μ_2	Insulin-independent glucose elimination rate
P	liver-glucose production rate due to glycemia
σ_1	Insulin release rate due to incretins hormones in the intestine
σ_2	Pancreatic insulin secretion rate
d_1	Insulin elimination rate
d_3	Decay rate of insulin due to glucagon concentration
σ_3	Pancreatic glucagon secretion rate
d_2	Glucagon elimination rate
d_4	Decay rate of glucagon due to insulin concentration
D	Dose of glucose

3. QUALITATIVE ANALYSIS

In this section, the model will be qualitatively examined [27]. Initially, an assessment will be made to determine the region in which the state variables exhibit positivity and finite values. Subsequently, the steady-state solutions of model (2.1) will be derived, and their stability will be analyzed. The subsequent subsections will present the primary findings.

3.1. **Positivity and boundedness.**

Theorem 3.1. *If* $(S(0), N(0), G(0), I(0), C(0)) \in R^5_{\geq 0}$ *then the set* Ω=$\{(S, N, G, I, C) \in R^5_{\geq 0} : 0 \leq S \leq D,\ 0 \leq N \leq \frac{\alpha D}{(\beta_1+\beta_2)}, 0 \leq G + I + C \leq [G(0) + I(0) + C(0) + (\beta_1 + \beta_2 + \sigma_1)\frac{\alpha D}{m(\beta_1+\beta_2)}]e^{mz}\}$ *is positively invariant for model (2.1), where* $z \in [0, T]$, T *is any positive number and* $m = max\{\sigma_2 + \sigma_3, P\}$.

Proof. First, we prove that the state variables are non-negative. Let $(S(0), N(0), G(0), I(0), C(0)) \in \Omega$. Rewrite the first equation in (2.1) as:

$$S' + \alpha S = 0. \tag{3.1}$$

Multiply both sides by $\exp\{\int_0^t \alpha\, du\}$ [28], then we can express (3.1) as:

$$\frac{d}{dt}\Big(S\ \exp\{\int_0^t \alpha\, du\}\Big) = 0. \tag{3.2}$$

The integration of (3.2) from 0 to t yields,

$$\Big[S\ \exp\{\int_0^t \alpha\, du\}\Big]_0^t = 0,$$

$$S(t)\ \exp\{\int_0^t \alpha\, du\} - S(0) = 0.$$

Hence,

$$S(t) = S(0)\ \exp\{-\int_0^t \alpha\, du\} \geq 0.$$

In a similar fashion, from the second equation in (2.1), we have

$$N' - \alpha S + (\beta_1 + \beta_2)N = 0,$$
$$N' - \Big[\alpha\frac{S}{N} - (\beta_1 + \beta_2)\Big]N = 0. \tag{3.3}$$

Multiply (3.3) by $\exp\{-\int_0^t \Big[\alpha\frac{S}{N} - (\beta_1 + \beta_2)\Big]\, du\}$, we obtain

$$\frac{d}{dt}\Big(N\ \exp\{-\int_0^t \Big[\alpha\frac{S}{N} - (\beta_1 + \beta_2)\Big]\, du\}\Big) = 0. \tag{3.4}$$

Integrating both sides of (3.4) from 0 to t,

$$\Big[N\ \exp\{-\int_0^t \Big[\alpha\frac{S}{N} - (\beta_1 + \beta_2)\Big]\, du\}\Big]_0^t = 0,$$
$$N(t)\ \exp\{-\int_0^t \Big[\alpha\frac{S}{N} - (\beta_1 + \beta_2)\Big]\, du\} - N(0) = 0.$$

Hence,

$$N(t) = N(0)\ exp\{\int_0^t \Big[\alpha\frac{S}{N} - (\beta_1 + \beta_2)\Big]\, du\} \geq 0.$$

In the same way, we can prove that $G(t), I(t),$ and $C(t)$ are non-negative. Thus, all non-negative solutions initiated in Ω remain non-negative.

Next, we prove the boundedness of the solutions. By integrating both sides of the first equation in (2.1) from 0 to t, we obtain

$$\ln S(t) - \ln S(0) = -\alpha t.$$

Since $S(0) = D$, then

$$S(t) = De^{-\alpha t} \leq D.$$

Similarly, the second equation in (2.1) becomes

$$N' \leq \alpha D - (\beta_1 + \beta_2)N,$$
$$N' + (\beta_1 + \beta_2)N \leq \alpha D.$$

Solving for $N(t)$ [28], we have

$$\frac{d}{dt}(e^{(\beta_1+\beta_2)t}N) \leq \alpha D e^{(\beta_1+\beta_2)t},$$
$$N(t) \leq \frac{\alpha D}{\beta_1 + \beta_2} + N(0)e^{-(\beta_1+\beta_2)t}.$$

Thus,

$$\lim_{t\to\infty} \sup N(t) \leq \frac{\alpha D}{\beta_1 + \beta_2}.$$

Adding the third, fourth, and fifth equations in (2.1), we have

$$G' + I' + C' = (\beta_1 + \beta_2)N - \mu_1 GI - \mu_2 G + PC + \sigma_1 N + \sigma_2 G - d_1 I - d_3 C + \sigma_3 G - d_2 C - d_4 I,$$
$$G' + I' + C' \leq (\beta_1 + \beta_2 + \sigma_1)N + (\sigma_2 + \sigma_3)G + PC.$$

Let $m = max\{\sigma_2 + \sigma_3, P\}$, then

$$\begin{aligned} G' + I' + C' &\leq (\beta_1 + \beta_2 + \sigma_1)\frac{\alpha D}{\beta_1 + \beta_2} + (\sigma_2 + \sigma_3)G + PC + mI, \\ &\leq (\beta_1 + \beta_2 + \sigma_1)\frac{\alpha D}{\beta_1 + \beta_2} + m(G + C + I), \end{aligned}$$

that is,

$$(G+I+C)' - m(G+I+C) \leq (\beta_1+\beta_2+\sigma_1)\frac{\alpha D}{\beta_1+\beta_2}.$$

Again, using the integrating factor method [28], we obtain

$$\frac{d}{dt}(e^{-mt}(G+I+C)) \leq (\beta_1+\beta_2+\sigma_1)\frac{\alpha D}{\beta_1+\beta_2}e^{-mt}.$$

Integrating both sides from 0 to t, we get

$$G(t)+I(t)+C(t) \leq [G(0)+I(0)+C(0)+(\beta_1+\beta_2+\sigma_1)\frac{\alpha D}{m(\beta_1+\beta_2)}]e^{mz},$$

where $z \in [0,T]$, and T is any positive number.

Hence, all solutions of model (2.1) are bounded and non-negative. Therefore, Ω is positively invariant. □

3.2. **Steady-state solution.** We can explore the steady-state solutions of (2.1), which is referred as the equilibrium points of the system, by setting the rates of the equations in (2.1) to zero [27], that is,

$$-\alpha S = 0, \tag{3.5}$$
$$\alpha S - (\beta_1+\beta_2)N = 0, \tag{3.6}$$
$$(\beta_1+\beta_2)N - \mu_1 GI - \mu_2 G + PC = 0, \tag{3.7}$$
$$\sigma_1 N + \sigma_2 G - d_1 I - d_3 C = 0, \tag{3.8}$$
$$\sigma_3 G - d_2 C - d_4 I = 0. \tag{3.9}$$

From equations (3.5) and (3.6), we obtain the equilibrium values for S and N, that is,

$$\begin{aligned} S^* &= 0, \\ N^* &= 0. \end{aligned} \tag{3.10}$$

Solving the equations (3.7), (3.8), and (3.9), we obtain the equilibrium values for $I,\ G$, and C,

$$\begin{aligned} I^* &= \frac{P\sigma_2}{d_3\mu_1} - \frac{Pd_1}{d_3\mu_1}\left(\frac{\sigma_2 d_2 - \sigma_3 d_3}{d_1 d_2 - d_3 d_4}\right) - \frac{\mu_2}{\mu_1}, \\ G^* &= \left(\frac{d_1 d_2 - d_3 d_4}{\sigma_2 d_2 - \sigma_3 d_3}\right) I^*, \\ C^* &= \left(\frac{\sigma_2}{d_3}\left(\frac{d_1 d_2 - d_3 d_4}{\sigma_2 d_2 - \sigma_3 d_3}\right) - \frac{d_1}{d_3}\right) I^*. \end{aligned} \tag{3.11}$$

For the equilibrium point to be biologically meaningful, it must be non-negative. Hence, we state the following theorem.

Theorem 3.2. *If* $\frac{P\sigma_2}{d_3\mu_1} > \left(\frac{Pd_1}{d_3\mu_1}\left(\frac{\sigma_2 d_2 - \sigma_3 d_3}{d_1 d_2 - d_3 d_4}\right) + \frac{\mu_2}{\mu_1}\right)$, $\sigma_2 d_2 > \sigma_3 d_3$, $d_1 d_2 > d_3 d_4$, *and* $\sigma_2(d_1 d_2 - d_3 d_4) > d_1(\sigma_2 d_2 - \sigma_3 d_3)$, *then model (2.1) has a unique equilibrium point,* $E = (0, 0, G^*, I^*, C^*)$, *where* $G^*,\ I^*$, *and* C^* *are given in* (3.11).

3.3. **Stability of equilibrium.** The local stability of the steady-state solution is investigated using the linearization method, and the global stability is examined using Lyapunov functions [27].

Theorem 3.3. *If the equilibrium point* $E = (0, 0, G^*, I^*, C^*)$ *exists, it is locally asymptotically stable when* $\mu_2(d_1 + d_2) \geq P\sigma_3$, *and* $(\mu_2 d_1 d_2 + \mu_1\sigma_2 d_2 G^* + P\sigma_2 d_4) > \sigma_3(\mu_1 d_3 G^* + Pd_1)$.

Proof. The Jacobian matrix of model (2.1) at E is given by

$$J(E) = \begin{bmatrix} -\alpha & 0 & 0 & 0 & 0 \\ \alpha & -(\beta_1+\beta_2) & 0 & 0 & 0 \\ 0 & (\beta_1+\beta_2) & -\mu_1 I^* - \mu_2 & -\mu_1 G^* & P \\ 0 & \sigma_1 & \sigma_2 & -d_1 & -d_3 \\ 0 & 0 & \sigma_3 & -d_4 & -d_2 \end{bmatrix}.$$

Solving the characteristic equation $|J(E) - \lambda I| = 0$, we get the eigenvalues, $\lambda_1 = -\alpha$, $\lambda_2 = -(\beta_1+\beta_2)$, which are both negative, however $\lambda_{3,4,5}$ satisfy the following equation:

$$a_3\lambda^3 + a_2\lambda^2 + a_1\lambda + a_0 = 0,$$

where,

$$\begin{aligned} a_3 &= 1, \\ a_2 &= \mu_1 I^* + \mu_2 + d_1 + d_2, \\ a_1 &= \mu_1 d_1 I^* + \mu_1 d_2 I^* + \mu_1 G^* \sigma_2 - P\sigma_3 + \mu_2 d_1 + \mu_2 d_2 + d_1 d_2 - d_3 d_4, \\ a_0 &= \mu_1 d_1 d_2 I^* - \mu_1 I^* d_3 d_4 - \mu_1 G^* \sigma_3 d_3 + \mu_1 \sigma_2 d_2 G^* - P\sigma_3 d_1 + P\sigma_2 d_4 + \mu_2 d_1 d_2 - \mu_2 d_3 d_4. \end{aligned}$$

In order to find the signs of $\lambda_{3,4,5}$, we use Descartes' rule of signs [29], $\lambda_{3,4,5}$ are negative if $a_{0,1,2,3} > 0$. Clearly, $a_2 > 0$, and $a_3 > 0$. To get $a_1 > 0$ we must have $d_1 d_2 > d_3 d_4$, and $\mu_2(d_1+d_2) \geq P\sigma_3$, and to get $a_0 > 0$ we must have $d_1 d_2 > d_3 d_4$, and $(\mu_2 d_1 d_2 + \mu_1 \sigma_2 d_2 G^* + P\sigma_2 d_4) > \sigma_3(\mu_1 d_3 G^* + P d_1)$. Hence, the equilibrium point, E is locally asymptotically stable if $\mu_2(d_1+d_2) \geq P\sigma_3$, and $(\mu_2 d_1 d_2 + \mu_1 \sigma_2 d_2 G^* + P\sigma_2 d_4) > \sigma_3(\mu_1 d_3 G^* + P d_1)$. □

Theorem 3.4. *The equilibrium point $E = (0, 0, G^*, I^*, C^*)$ is globally asymptotically stable if $4d_1 d_2 \mu_2 > 6(d_1 P\sigma_3 + \mu_2 d_3 d_4)$.*

Proof. Define the Lyapunov function as

$$L(S, N, G, I, C) = A_1 S + A_2 N + \frac{A_3}{2}(G - G^*)^2 + \frac{A_4}{2}(I - I^*)^2 + \frac{A_5}{2}(C - C^*)^2, \tag{3.12}$$

where $A_1,\ A_2,\ A_3,\ A_4$ and A_5 are positive defined as follows

$$A_1 = A_2 = \frac{1}{(\beta_1+\beta_2)}\left(\frac{3(\beta_1+\beta_2)^2}{4\mu_2}A_3 + \frac{3\sigma_1^2}{4d_1}\right), \tag{3.13}$$

$$A_3 = \frac{-b_1 + \sqrt{b_1^2 - 4a_1 c_1}}{2a_1}, \tag{3.14}$$

$$A_4 = 1, \tag{3.15}$$

$$A_5 = \frac{-b_2 + \sqrt{b_2^2 - 4a_2 c_2}}{2a_2}, \tag{3.16}$$

and

$$a_1 = \mu_1^2 G^{*2}, \quad b_1 = -(2\mu_1\sigma_2 G^* + \frac{4}{9}\mu_2 d_1), \quad c_1 = \sigma_2^2, \tag{3.17}$$

$$a_2 = 3d_1\sigma_3^2 + 3A_3\mu_2 d_4^2, \tag{3.18}$$

$$b_2 = (-4d_1 d_2 \mu_2 + 6(d_1 P\sigma_3 + \mu_2 d_3 d_4))A_3, \tag{3.19}$$

$$c_2 = 3A_3^2 d_1 P^2 + 3A_3\mu_2 d_3^2. \tag{3.20}$$

It is easy to show that L is a positive definite function. Evaluating the derivative of L, we obtain

$$L' = A_1 S' + A_2 N' + A_3(G - G^*)G' + A_4(I - I^*)I' + A_5(C - C^*)C'.$$

Along the solution of model (2.1) and employing equations (3.7)-(3.9) at the equilibrium E, we have

$$\begin{aligned}L' =& - A_1\alpha S + A_2\alpha S - A_2(\beta_1+\beta_2)N + A_3(G-G^*)[(\beta_1+\beta_2)N - \mu_1 GI - \mu_2 G + PC\\ &+ \mu_1 G^*I^* + \mu_2 G^* - PC^*] + A_4(I-I^*)[\sigma_1 N + \sigma_2 G - d_1 I - d_3 C - \sigma_2 G^* + d_1 I^* + d_3 C^*]\\ &+ A_5(C-C^*)[\sigma_3 G - d_2 C - d_4 I - \sigma_3 G^* + d_2 C^* + d_4 I^*].\end{aligned}$$

Rearranging the terms and noting that $A_1 = A_2$ and $A_4 = 1$, we get

$$\begin{aligned}L' =& - A_2(\beta_1+\beta_2)N + A_3(\beta_1+\beta_2)(G-G^*)N + \sigma_1(I-I^*)N - A_3\mu_1(G-G^*)(GI - G^*I^*)\\ &- A_3\mu_2(G-G^*)^2 + A_3P(G-G^*)(C-C^*) + \sigma_2(I-I^*)(G-G^*) - d_1(I-I^*)^2\\ &- d_3(I-I^*)(C-C^*) + A_5\sigma_3(C-C^*)(G-G^*) - A_5d_2(C-C^*)^2 - A_5d_4(C-C^*)(I-I^*).\end{aligned}$$

Rewriting $GI - G^*I^* = GI - G^*I + G^*I - G^*I^* = (G-G^*)I + (I-I^*)G^*$ and collecting terms, we obtain

$$\begin{aligned}L' =& - A_2(\beta_1+\beta_2)N + A_3(\beta_1+\beta_2)(G-G^*)N + \sigma_1(I-I^*)N - A_3\mu_1(G-G^*)^2 I\\ &- (A_3\mu_1 G^* - \sigma_2)(G-G^*)(I-I^*) - A_3\mu_2(G-G^*)^2 + (A_3P + A_5\sigma_3)(G-G^*)(C-C^*)\\ &- (d_3 + A_5d_4)(C-C^*)(I-I^*) - d_1(I-I^*)^2 - A_5d_2(C-C^*)^2.\end{aligned}$$

Equivalently,

$$\begin{aligned}L' =& - A_2(\beta_1+\beta_2)N + A_3(\beta_1+\beta_2)(G-G^*)N + \sigma_1(I-I^*)N - A_3\mu_1(G-G^*)^2 I\\ &- (A_3\mu_1 G^* - \sigma_2)(G-G^*)(I-I^*) - \frac{A_3\mu_2}{3}(G-G^*)^2 - \frac{A_3\mu_2}{3}(G-G^*)^2 - \frac{A_3\mu_2}{3}(G-G^*)^2\\ &+ (A_3P + A_5\sigma_3)(G-G^*)(C-C^*) - (d_3 + A_5d_4)(C-C^*)(I-I^*) - \frac{d_1}{3}(I-I^*)^2\\ &- \frac{d_1}{3}(I-I^*)^2 - \frac{d_1}{3}(I-I^*)^2 - A_5d_2(C-C^*)^2.\end{aligned}$$

Next, we complete the squares in the terms,

$$\begin{aligned}L' =& N\Bigg\{ - A_2(\beta_1+\beta_2) - \frac{A_3\mu_2}{3}\Bigg[(G-G^*)^2 - \frac{3}{\mu_2}(\beta_1+\beta_2)(G-G^*) + (\frac{3}{2\mu_2}(\beta_1+\beta_2))^2\\ &- (\frac{3}{2\mu_2}(\beta_1+\beta_2))^2\Bigg] - \frac{d_1}{3}\Bigg[(I-I^*)^2 - \frac{3\sigma_1}{d_1}(I-I^*) + (\frac{3\sigma_1}{2d_1})^2 - (\frac{3\sigma_1}{2d_1})^2\Bigg]\Bigg\} - A_3\mu_1(G-G^*)^2 I\\ &- \frac{A_3\mu_2}{3}\Bigg[(G-G^*)^2 + \frac{3(A_3\mu_1G^* - \sigma_2)}{A_3\mu_2}(G-G^*)(I-I^*) + \left(\frac{3(A_3\mu_1G^* - \sigma_2)}{2A_3\mu_2}\right)^2(I-I^*)^2\\ &- \left(\frac{3(A_3\mu_1G^* - \sigma_2)}{2A_3\mu_2}\right)^2(I-I^*)^2\Bigg] - \frac{d_1}{3}(I-I^*)^2 - \frac{A_3\mu_2}{3}\Bigg[(G-G^*)^2\\ &- \frac{3(A_3P + A_5\sigma_3)}{A_3\mu_2}(G-G^*)(C-C^*) + \left(\frac{3(A_3P + A_5\sigma_3)}{2A_3\mu_2}\right)^2(C-C^*)^2\\ &- \left(\frac{3(A_3P + A_5\sigma_3)}{2A_3\mu_2}\right)^2(C-C^*)^2\Bigg] - \frac{d_1}{3}\Bigg[(I-I^*)^2 + \frac{3(d_3+A_5d_4)}{d_1}(I-I^*)(C-C^*)\\ &+ \left(\frac{3(d_3+A_5d_4)}{2d_1}\right)^2(C-C^*)^2 - \left(\frac{3(d_3+A_5d_4)}{2d_1}\right)^2(C-C^*)^2\Bigg] - A_5d_2(C-C^*)^2.\end{aligned}$$

Collecting the terms again, we get

$$\begin{aligned}L' =& N\Bigg\{ - A_2(\beta_1+\beta_2) - \frac{A_3\mu_2}{3}\left[(G-G^*) - \frac{3}{2\mu_2}(\beta_1+\beta_2)^2\right]^2 + \frac{3A_3}{4\mu_2}(\beta_1+\beta_2)^2\\ &- \frac{d_1}{3}\left[(I-I^*) - \frac{3\sigma_1}{2d_1}\right]^2 + \frac{3\sigma_1^2}{4d_1}\Bigg\} - A_3\mu_1(G-G^*)^2 I\end{aligned}$$

$$
\begin{aligned}
&- \frac{A_3\mu_2}{3}\left[(G-G^*)+\frac{3(A_3\mu_1G^*-\sigma_2)}{2A_3\mu_2}(I-I^*)\right]^2+\left[\frac{3(A_3\mu_1G^*-\sigma_2)^2}{4A_3\mu_2}-\frac{d_1}{3}\right](I-I^*)^2\\
&- \frac{A_3\mu_2}{3}\left[(G-G^*)-\frac{3(A_3P+A_5\sigma_3)}{2A_3\mu_2}(C-C^*)\right]^2-\frac{d_1}{3}\left[(I-I^*)+\frac{3(d_3+A_5d_4)}{2d_1}(C-C^*)\right]^2\\
&+\left[\frac{3(A_3P+A_5\sigma_3)^2}{4A_3\mu_2}+\frac{3(d_3+A_5d_4)^2}{4d_1}-A_5d_2\right](C-C^*)^2.
\end{aligned}
$$

For L' to be negative, we must show that

$$-A_2(\beta_1+\beta_2)+\frac{3A_3}{4\mu_2}(\beta_1+\beta_2)^2+\frac{3\sigma_1^2}{4d_1}=0, \tag{3.21}$$

$$\frac{3(A_3\mu_1G^*-\sigma_2)^2}{4A_3\mu_2}-\frac{d_1}{3}=0, \tag{3.22}$$

$$\frac{3(A_3P+A_5\sigma_3)^2}{4A_3\mu_2}+\frac{3(d_3+A_5d_4)^2}{4d_1}-A_5d_2=0. \tag{3.23}$$

Rearranging equation (3.22), we obtain

$$\mu_1^2G^{*2}A_3^2-(2\mu_1\sigma_2G^*+\frac{4}{9}\mu_2d_1)A_3+\sigma_2^2=0,$$

Solving for A_3, we have

$$
\begin{aligned}
A_3=&\frac{-b_1+\sqrt{b_1^2-4a_1c_1}}{2a_1},\\
a_1=\mu_1^2G^{*2},\quad b_1=&-(2\mu_1\sigma_2G^*+\frac{4}{9}\mu_2d_1),\quad c_1=\sigma_2^2.
\end{aligned}
$$

Similarly, equation (3.23) becomes

$$(3d_1\sigma_3^2+3A_3\mu_2d_4^2)A_5^2-A_3(4d_1d_2\mu_2-6d_1P\sigma_3-6\mu_2d_3d_4)A_5+3A_3^2d_1P^2+3A_3\mu_2d_3^2=0.$$

Solving for A_5, we get

$$
\begin{aligned}
A_5=&\frac{-b_2+\sqrt{b_2^2-4a_2c_2}}{2a_2},\\
a_2=&3d_1\sigma_3^2+3A_3\mu_2d_4^2,\\
b_2=&(-4d_1d_2\mu_2+6(d_1P\sigma_3+\mu_2d_3d_4))A_3,\\
c_2=&3A_3^2d_1P^2+3A_3\mu_2d_3^2.
\end{aligned}
$$

Therefore, from (3.21), we find

$$A_2=\frac{1}{(\beta_1+\beta_2)}\left(\frac{3(\beta_1+\beta_2)^2}{4\mu_2}A_3+\frac{3\sigma_1^2}{4d_1}\right).$$

Clearly, A_3 and A_2 are positive. Also, A_5 is positive if $4d_1d_2\mu_2>6(d_1P\sigma_3+\mu_2d_3d_4)$. The obtained values of A_2, A_3 and A_5 are the same as in (3.13)-(3.16). Thus,

$$
\begin{aligned}
L'=&-\frac{A_3\mu_2}{3}\left[(G-G^*)-\frac{3}{2\mu_2}(\beta_1+\beta_2)^2\right]^2N-\frac{d_1}{3}\left[(I-I^*)-\frac{3\sigma_1}{2d_1}\right]^2N-A_3\mu_1(G-G^*)^2I\\
&-\frac{A_3\mu_2}{3}\left[(G-G^*)+\frac{3(A_3\mu_1G^*-\sigma_2)}{2A_3\mu_2}(I-I^*)\right]^2\\
&-\frac{A_3\mu_2}{3}\left[(G-G^*)-\frac{3(A_3P+A_5\sigma_3)}{2A_3\mu_2}(C-C^*)\right]^2\\
&-\frac{d_1}{3}\left[(I-I^*)+\frac{3(d_3+A_5d_4)}{2d_1}(C-C^*)\right]^2.
\end{aligned}
$$

Hence, if $4d_1d_2\mu_2 > 6(d_1P\sigma_3 + \mu_2d_3d_4)$ then L' is negative, therefore, the equilibrium point E is globally asymptotically stable. □

The theoretical analysis of stability, particularly the establishment of global asymptotic stability, serves as a foundational step in validating the model's predictions. By demonstrating that the equilibrium point is both locally and globally stable, the study ensures that the system's behavior aligns with biological expectations of maintaining glucose homeostasis over time. This theoretical insight is further reinforced through numerical simulations, which consistently show that the model's solutions converge to the stable equilibrium point under various initial conditions.

4. Numerical Analysis

This section presents the numerical results of model (2.1) obtained by solving the equations through the MATLAB solver ode45. Various experimental simulations of the model are depicted. Moreover, we analyze parameter sensitivity to attain a comprehensive understanding of the essential factors that may contribute to the development of the most effective therapeutic strategies.

4.1. **Numerical experiments.** We solve model (2.1) numerically with the following different initial values:
(a) $G(0)$ = 0.7, $I(0)$ = 0.5, $C(0)$ = 0.3, $N(0)$=0, $S(0) = D$;
(b) $G(0)$ = 0.5, $I(0)$ = 0.5, $C(0)$ = 0.5, $N(0)$=0, $S(0) = D$;
(c) $G(0)$ = 0.3, $I(0)$ = 0.5, $C(0)$ = 0.7, $N(0)$=0, $S(0) = D$.
The parameter values are displayed in Table 2. They are estimated to satisfy the existence and stability conditions of the equilibrium derived from the qualitative analysis.

Table 2. The model parameter values.

Parameter	Value	Unit
S	-	mM
N	-	mM
G	-	mM
I	-	mM
G	-	mM
α	5×10^{-2}	min^{-1}
β_1	4×10^{-2}	min^{-1}
β_2	2×10^{-2}	min^{-1}
μ_1	7×10^{-2}	$min^{-1}mM^{-1}$
μ_2	3×10^{-2}	min^{-1}
P	4×10^{-2}	min^{-1}
σ_1	2×10^{-2}	min^{-1}
σ_2	2×10^{-2}	min^{-1}
d_1	2×10^{-2}	min^{-1}
d_3	5×10^{-3}	min^{-1}
σ_3	3×10^{-2}	min^{-1}
d_2	2×10^{-2}	min^{-1}
d_4	5×10^{-3}	min^{-1}
D	5	mM

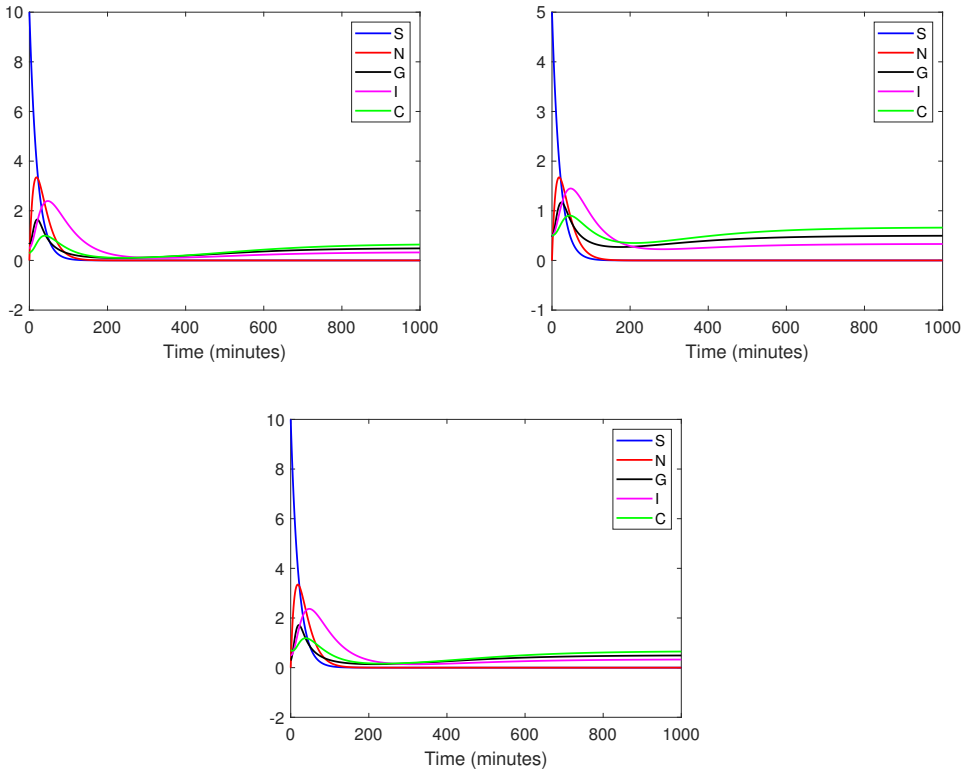

FIGURE 2. Time variations of S, N, G, I, and C with parameter values from Table 2 and initial conditions (a)-(c).

We observe in Figure 2 that, for different initial conditions, the numerical solutions eventually converge to the equilibrium point E. In particular, the equilibrium points in the above experiments are the following: $E_a = (0, 0, 0.4851, 0.3220, 0.6394)$, $E_b = (0, 0, 0.4966, 0.3308, 0.6605)$, and $E_c = (0, 0, 0.4902, 0.3259, 0.6487)$ where they agree with the qualitative equilibrium point $E = (0, 0, 0.5, 0.3333, 0.6667)$. This means that the equilibrium point is stable, which is consistent with the qualitative results. The agreement between the analytical stability results and the numerical experiments underscores the model's reliability and robustness in capturing the dynamics of glucose, insulin, and glucagon interactions. This bridging of theory and simulation not only validates the model's predictions but also underscores its potential as a tool for understanding long-term physiological behavior and designing effective therapeutic strategies.

4.2. **Parameters analysis.** We investigate how the parameters in model (2.1) relate to the variable G, representing plasma glucose concentration, using numerical methods. The findings are illustrated in Figure 3, which demonstrates significant implications for understanding the biological roles of insulin and glucagon in glucose regulation.

Insulin plays a crucial role in regulating plasma glucose levels through multiple mechanisms. The release of insulin is influenced by incretin hormones in the intestine (σ_1) and the pancreatic insulin secretion rate (σ_2), both of which decrease plasma glucose concentration by facilitating glucose uptake. Insulin-dependent (μ_1) and insulin-independent (μ_2) glucose elimination rates further contribute to lowering glucose levels. Conversely, insulin increases plasma glucose concentration by enhancing the insulin elimination rate (d_1) and promoting insulin decay due to glucagon's presence (d_3). These dynamics highlight insulin's dual role in glucose regulation, balancing glucose uptake and elimination.

Glucagon, on the other hand, acts as a counter-regulatory hormone to insulin, promoting an increase in plasma glucose concentration. It achieves this by stimulating liver glucose production (P) and pancreatic glucagon secretion (σ_3), which are critical during hypoglycemic conditions. However, glucagon also decreases plasma glucose concentration through its elimination rate (d_2) and decay rate due to insulin (d_4). This interplay between glucagon and insulin underscores the complexity of glucose homeostasis, where both hormones work in tandem to maintain stable glucose levels.

Additionally, glucose concentration is directly influenced by the glucose transfer rate from the stomach to the intestine (α). The comparison between the glucose transfer rate from the jejunum to plasma (β_1) and the glucose transfer rate from the ileum to plasma (β_2) reveals that higher β_1 values lead to faster plasma glucose elevation. In contrast, higher β_2 values result in slower glucose absorption. This insight emphasizes the importance of understanding glucose absorption dynamics for maintaining healthy glucose levels.

The biological interpretation of these parameter dynamics provides a comprehensive understanding of how insulin and glucagon regulate glucose levels in the human body. These findings could inform therapeutic strategies aimed at optimizing glucose regulation in individuals with metabolic disorders.

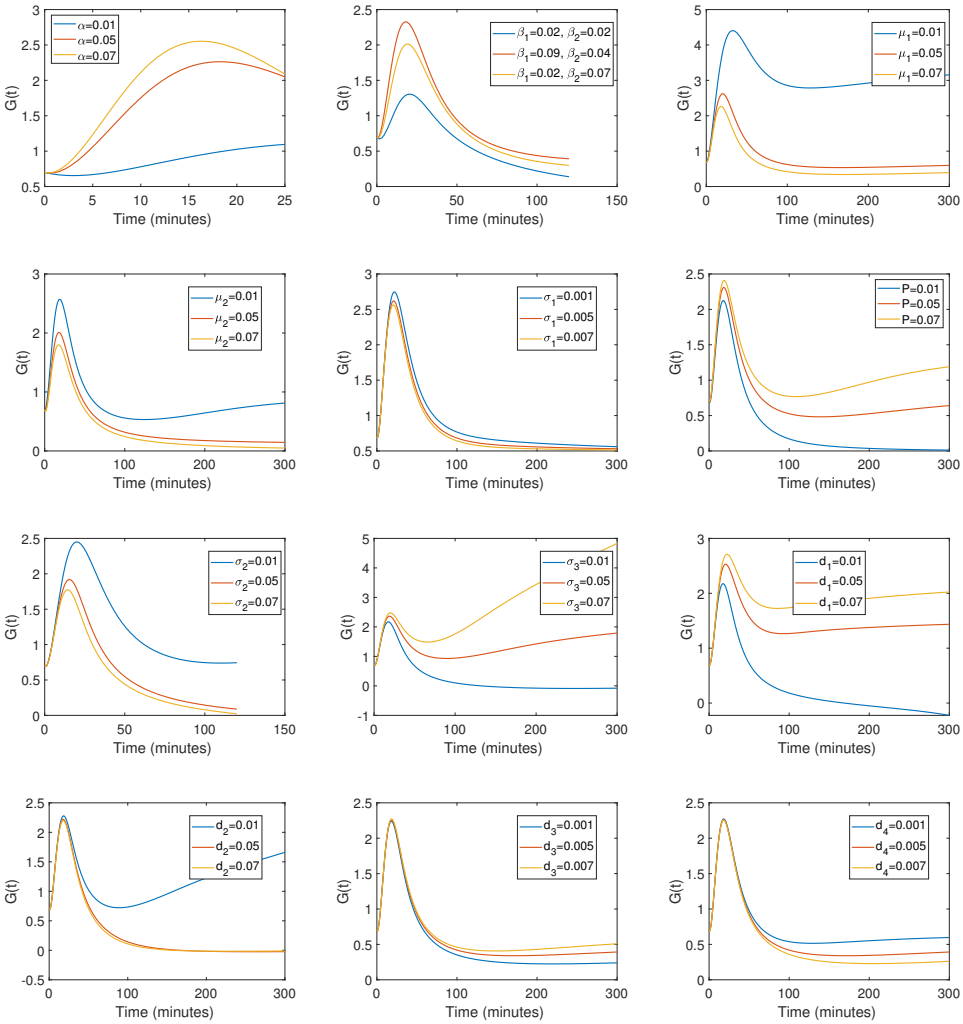

FIGURE 3. The relationship between G and the parameters in model (2.1).

4.3. **Sensitivity analysis.** We seek to analyze the sensitivity of G^* to the parameters in model (2.1). To achieve this goal, we are utilizing both analytical and numerical methods. In the analytical approach, we investigate the sensitivity of equilibrium values by evaluating the changes that occur in the equilibrium value when a parameter is altered. For instance, we are calculating $\frac{\partial G^*}{\partial \delta}$, where δ represents any parameter in model (2.1). In the numerical approach, all parameters except one are held constant, and the changes in the equilibrium value with respect to the variation of this parameter are plotted.

Our analysis aims to provide an in-depth understanding of how variations in the parameters impact the equilibrium glucose level.

We start the sensitivity analysis with the analytical approach. The changes of the equilibrium value G^* with respect to the parameters in the model are demonstrated below.

$$\begin{aligned}
\frac{\partial G^*}{\partial \mu_1} &= \frac{Pd_1}{d_3\mu_1^2} + (\frac{\mu_2}{\mu_1^2} - \frac{P\sigma_2}{d_3\mu_1^2})(\frac{d_1d_2 - d_3d_3}{\sigma_2d_2 - \sigma_3d_3}) < 0,\\
\frac{\partial G^*}{\partial \mu_2} &= -\frac{1}{\mu_1}(\frac{d_1d_2 - d_3d_3}{\sigma_2d_2 - \sigma_3d_3}) < 0,\\
\frac{\partial G^*}{\partial P} &= \frac{\sigma_2}{d_3\mu_1}(\frac{d_1d_2 - d_3d_3}{\sigma_2d_2 - \sigma_3d_3}) - \frac{d_1}{d_3\mu_1} > 0,\\
\frac{\partial G^*}{\partial \sigma_2} &= \frac{-d_2(d_1d_2 - d_3d_4)}{(\sigma_2d_2 - \sigma_3d_3)^2}I^* + (\frac{d_1d_2 - d_3d_4}{\sigma_2d_2 - \sigma_3d_3})\frac{\partial I^*}{\partial \sigma_2} < 0,\\
\frac{\partial G^*}{\partial \sigma_3} &= (\frac{d_3(d_1d_2 - d_3d_4)}{(\sigma_2d_2 - \sigma_3d_3)^2})I^* + (\frac{d_1d_2 - d_3d_4}{\sigma_2d_2 - \sigma_3d_3})\frac{\partial I^*}{\partial \sigma_3} > 0,\\
\frac{\partial G^*}{\partial d_1} &= \frac{d_2}{(\sigma_2d_2 - \sigma_3d_3)}I^* + (\frac{d_1d_2 - d_3d_4}{\sigma_2d_2 - \sigma_3d_3})\frac{\partial I^*}{\partial d_1} > 0,\\
\frac{\partial G^*}{\partial d_4} &= \frac{-d_3}{(\sigma_2d_2 - \sigma_3d_3)}I^* + (\frac{d_1d_2 - d_3d_4}{\sigma_2d_2 - \sigma_3d_3})\frac{\partial I^*}{\partial d_4} < 0,\\
\frac{\partial G^*}{\partial d_3} &= \frac{d_2(\sigma_3d_1 - \sigma_2d_4)}{(\sigma_2d_2 - \sigma_3d_3)^2}I^* + (\frac{d_1d_2 - d_3d_4}{\sigma_2d_2 - \sigma_3d_3})\frac{\partial I^*}{\partial d_3},\\
\frac{\partial G^*}{\partial d_2} &= \frac{-d_3(\sigma_3d_1 - \sigma_2d_4)}{(\sigma_2d_2 - \sigma_3d_3)^2}I^* + (\frac{d_1d_2 - d_3d_4}{\sigma_2d_2 - \sigma_3d_3})\frac{\partial I^*}{\partial d_2}.
\end{aligned} \tag{4.1}$$

Noting that,

$$\begin{aligned}
\frac{\partial I^*}{\partial \sigma_2} &= \frac{P}{d_3\mu_1}(1 - \frac{d_1d_2}{d_1d_2 - d_3d_4}) < 0,\\
\frac{\partial I^*}{\partial \sigma_3} &= \frac{Pd_1}{\mu_1(d_1d_2 - d_3d_4)} > 0,\\
\frac{\partial I^*}{\partial d_1} &= \frac{Pd_4}{\mu_1}\left[\frac{\sigma_2d_2 - \sigma_3d_3}{(d_1d_2 - d_3d_4)^2}\right] > 0,\\
\frac{\partial I^*}{\partial d_4} &= \frac{-Pd_1}{\mu_1}\left[\frac{\sigma_2d_2 - \sigma_3d_3}{(d_1d_2 - d_3d_4)^2}\right] < 0,\\
\frac{\partial I^*}{\partial d_3} &= \frac{Pd_4}{\mu_1}\left[\frac{\sigma_3d_1 - \sigma_2d_4}{(d_1d_2 - d_3d_4)^2}\right],\\
\frac{\partial I^*}{\partial d_2} &= \frac{-Pd_1}{\mu_1}\left[\frac{\sigma_3d_1 - \sigma_2d_4}{(d_1d_2 - d_3d_4)^2}\right].
\end{aligned} \tag{4.2}$$

Equation (4.1) demonstrates that when either the insulin-dependent (μ_1) or insulin-independent (μ_2) glucose elimination rate increases, or when the pancreatic insulin secretion rate (σ_2) increases, the glucose equilibrium levels (G^*) decrease. Conversely, when the insulin elimination rate (d_1) increases, G^* increases. This emphasizes insulin's crucial role in glucose regulation, highlighting its function in facilitating glucose

uptake and maintaining lower plasma glucose levels. It also suggests that faster insulin clearance can result in higher plasma glucose levels.

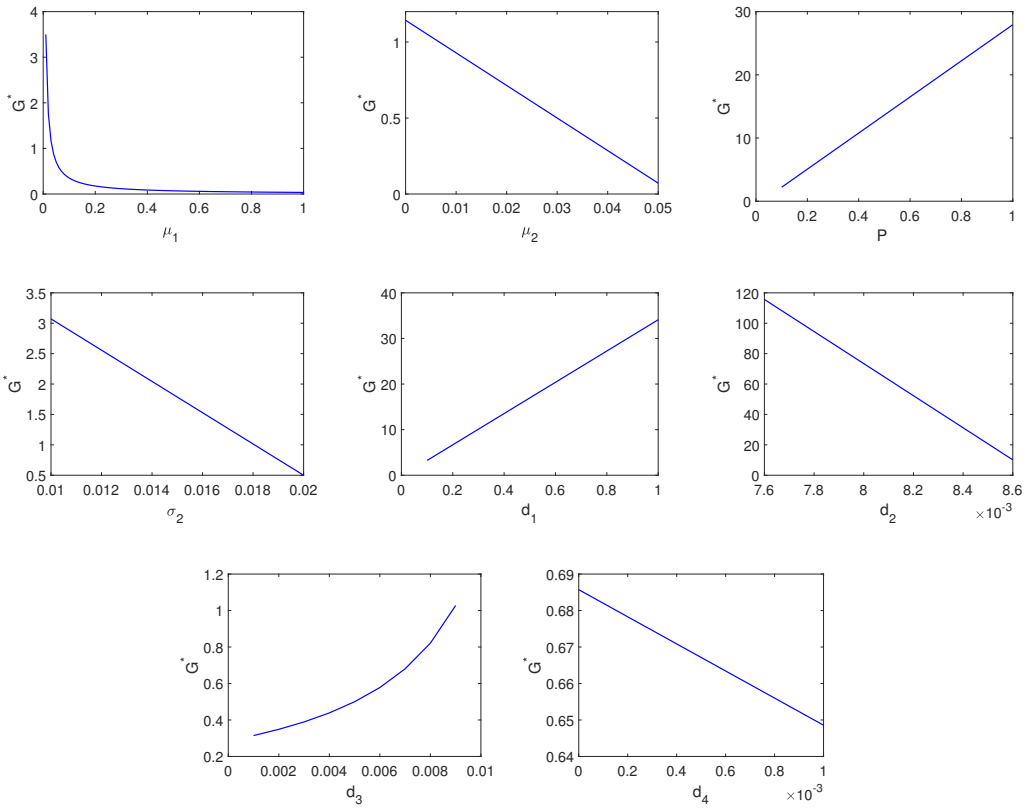

FIGURE 4. The sensitivity of G^* to the most effective parameters for model (2.1).

Moreover, if either the liver-glucose production rate (P) or the pancreatic glucagon secretion rate (σ_3) increases, G^* also increases. This reflects glucagon's role in elevating plasma glucose levels during hypoglycemia. However, if the decay rate of glucagon due to the presence of insulin (d_4) increases, G^* decreases. This demonstrates insulin's ability to suppress glucagon activity and lower glucose levels.
Additionally, the increase in the decay rate of insulin due to the presence of glucagon (d_3) has a dual impact on G^*. If the ratio of the pancreatic glucagon secretion rate (σ_3) to the pancreatic insulin secretion rate (σ_2) is higher than the ratio of the decay rate of glucagon due to the presence of insulin (d_4) to the insulin elimination rate (d_1), then G^* increases. Alternatively, if the ratios are the opposite, G^* decreases.

Meanwhile, suppose the ratio of the insulin elimination rate (d_1) to the decay rate of glucagon due to the presence of insulin (d_4) is higher than the ratio of the pancreatic insulin secretion rate (σ_2) to the pancreatic glucagon secretion rate (σ_3). In that case, the increase in the glucagon elimination rate (d_2) leads to a decrease in G^*. On the other hand, if the ratios are reversed, G^* increases. These findings highlight the intricate interplay between glucose, insulin, and glucagon, demonstrating how specific parameters affect glucose equilibrium levels.

Next, we investigate the sensitivity of the model parameters through numerical analysis. Figure 4 depicts how the variation in model parameters can impact the value of G^*. Notably, the numerical results agree with the analytical results, highlighting the accuracy and reliability of the model.

The sensitivity analysis underlines insulin's pivotal role in regulating glucose levels. Increased insulin secretion or enhanced glucose elimination rates consistently lower G^*, demonstrating insulin's effectiveness in maintaining glucose homeostasis. Conversely, glucagon plays a critical role in elevating glucose levels during hypoglycemia, with its secretion and liver-glucose production rates significantly impacting G^*. The dual effects of insulin and glucagon decay rates further emphasize the complexity of their interactions. By identifying the most influential parameters, this analysis guides the optimization of therapeutic strategies that manage diabetes and other metabolic disorders.

5. Discussion and Conclusions

The regulation of blood glucose levels is a critical physiological process governed by the interplay of several hormones produced by the pancreas. Insulin facilitates glucose uptake into cells for energy production, while glucagon raises blood glucose levels by converting glycogen into glucose in the liver. The delicate balance between these hormones ensures that cells receive sufficient energy while preventing prolonged hyperglycemia. Disruptions in this balance can lead to metabolic disorders such as diabetes, which pose significant health and economic challenges globally.

This study aimed to develop a mathematical model to investigate the regulation of glucose levels in the human body and their interactions with insulin and glucagon. The model includes the effect of incretin hormones in the intestine on insulin release. By formulating a nonlinear system of ordinary differential equations, the study provided a robust framework for understanding the dynamics of glucose regulation.

Through qualitative analysis, the model demonstrated that the state variables remain positive and bounded, ensuring the system's biological relevance. A unique steady-state solution was derived, and its stability was analyzed. The results revealed that the equilibrium point exists under specific conditions and is both locally and globally asymptotically stable. Numerical simulations further validated these findings, showing that the solutions converge to the stable equilibrium point across various initial conditions.

Sensitivity analysis provided more profound insights into the intricate relationship between glucose, insulin, and glucagon. Analytical and numerical approaches revealed how variations in model parameters impact the equilibrium glucose level (G^*). For instance, an increase in insulin-dependent or insulin-independent glucose elimination rates, as well as pancreatic insulin secretion rates, decreases G^*. Conversely, an increase in liver-glucose production rates or pancreatic glucagon secretion rates raises G^*. The analysis also highlighted the dual impact of insulin's decay rate due to the presence of glucagon, which can either increase or decrease G^* depending on specific parameter ratios. These results underscore the complexity of glucose regulation and the critical roles of insulin and glucagon in maintaining homeostasis.

The findings of this study closely aligned with established biological behavior and clinical observations. For instance, the model demonstrated how insulin secretion decreases plasma glucose concentration through insulin-dependent and insulin-independent glucose elimination rates, which is consistent with the physiological role of insulin in promoting glucose uptake by cells. Similarly, the model highlighted glucagon's role in increasing plasma glucose concentration by stimulating liver glucose production, a well-documented biological process during hypoglycemia. The sensitivity analysis further emphasized the critical balance between insulin and glucagon, showing how changes in their secretion or elimination rates can significantly impact glucose equilibrium levels. These results align with clinical observations, where disruptions in insulin or glucagon dynamics are associated with conditions such as type 2 diabetes mellitus and hypoglycemia. By providing a mathematical framework that captures these interactions, the model offers valuable insights into the mechanisms underlying glucose regulation and potential therapeutic targets.

The study uniquely combined equilibrium stability analysis with sensitivity analysis to investigate the impact of key parameters on glucose equilibrium levels. This dual focus enabled a deeper exploration of

the mechanisms underlying glucose homeostasis, highlighting the intricate interplay between insulin and glucagon.

While the model offers valuable insights, it is limited to the interactions between glucose, insulin, and glucagon, excluding other hormones such as somatostatin and amylin, as well as external factors like stress, physical activity, and diet, which also influence glucose homeostasis.

In conclusion, this study provided a comprehensive mathematical framework for understanding the complex dynamics of glucose regulation in the human body. The findings could serve as a foundation for developing more effective treatments for diabetes and other metabolic disorders.

Future research may expand the model to include additional hormones and external factors. Additionally, exploring the discrete-time counterpart of the model would enable the examination of its dynamical behavior in scenarios where data are collected at discrete intervals, such as in clinical or experimental settings. Numerical analysis of the discrete-time model could reveal new patterns and behaviors, further enhancing the understanding of glucose regulation and its applications in therapeutic strategies.

Competing interests. The authors declare no competing interests.

REFERENCES

[1] A.L. Morris, S.S. Mohiuddin, Biochemistry, Nutrients, StatPearls Publishing, 2025.

[2] R. Basiri, L.J. Cheskin, Enhancing the Impact of Individualized Nutrition Therapy with Real-Time Continuous Glucose Monitoring Feedback in Overweight and Obese Individuals with Prediabetes, Nutrients 16 (2024), 4005. https://doi.org/10.3390/nu16234005.

[3] A.M. Bell, How Insulin and Glucagon Regulate Blood Sugar, Medical News Today, 2023. https://www.medicalnewstoday.com/articles/316427.

[4] P.V. Röder, B. Wu, Y. Liu, W. Han, Pancreatic Regulation of Glucose Homeostasis, Exp. Mol. Med. 48 (2016), e219. https://doi.org/10.1038/emm.2016.6.

[5] H. Wang, J. Li, Y. kuang, Mathematical Modeling and Qualitative Analysis of Insulin Therapies, Math. Biosci. 210 (2007), 17–33. https://doi.org/10.1016/j.mbs.2007.05.008.

[6] B. Huard, A. Bridgewater, M. Angelova, Mathematical Investigation of Diabetically Impaired Ultradian Oscillations in the Glucose–Insulin Regulation, J. Theor. Biol. 418 (2017), 66–76. https://doi.org/10.1016/j.jtbi.2017.01.039.

[7] S. Saber, E. Bashier, S. Alzahrani, I. Noaman, A Mathematical Model of Glucose-Insulin Interaction with Time Delay, J. Appl. Comput. Math. 7 (2018), 3. https://doi.org/10.4172/2168-9679.1000416.

[8] M. Ma, J. Li, Dynamics of a Glucose–Insulin Model, J. Biol. Dyn. 16 (2022), 733–745. https://doi.org/10.1080/17513758.2022.2146769.

[9] S. Rathee, R. Nilam, M.E. Alexander, The Effects of Vitamin D on Glucose-Insulin Dynamics: Mathematical Model and Simulation, J. Diabetes Metab. Disord. Control. 8 (2021), 105–114. https://doi.org/10.15406/jdmdc.2021.08.00229.

[10] K. Saranya, T. Iswarya, V. Mohan, K.E. Sathappan, L. Rajendran, Mathematical modeling of Glucose, Insulin, β-Cell Mass: Homotopy Perturbation Method Approach, Eur. J. Mol. Clin. Med. 7 (2020), 3513–3530.

[11] S. Chowdhury, S.K. Manna, S. Roychowdhury, I. Chaudhuri, Mathematical Model of Ingested Glucose in Glucose-Insulin Regulation, J. Appl. Comput. Math. 3 (2020), 1–12.

[12] A. Devi, R. Kalita, A. Ghosh, A Mathematical Model of Glucose-Insulin Regulation Under the Influence of Externally Ingested Glucose (G-I-E Model), Int. J. Math. Stat. Invent. 4 (2016), 54–58.

[13] C. Eberle, W. Palinski, C. Ament, A Novel Mathematical Model Detecting Early Individual Changes of Insulin Resistance, Diabetes Technol. Ther. 15 (2013), 870–880. https://doi.org/10.1089/dia.2013.0084.

[14] M. Lombarte, M. Lupo, G. Campetelli, M. Basualdo, A. Rigalli, Mathematical Model of Glucose–Insulin Homeostasis in Healthy Rats, Math. Biosci. 245 (2013), 269–277. https://doi.org/10.1016/j.mbs.2013.07.017.

[15] A. De Gaetano, S. Panunzi, A. Matone, A. Samson, J. Vrbikova, et al., Routine OGTT: A Robust Model Including Incretin Effect for Precise Identification of Insulin Sensitivity and Secretion in a Single Individual, PLoS ONE 8 (2013), e70875. https://doi.org/10.1371/journal.pone.0070875.

[16] C. Li, Y. Liu, Y. Wang, X. Feng, Dynamic Modeling of the Glucose–Insulin System with Inhibitors Impulsive Control, Math. Methods Appl. Sci. (2024). https://doi.org/10.1002/mma.10266.

[17] M. Farman, A. Ahmad, A. Zehra, K.S. Nisar, E. Hincal, et al., Analysis and Controllability of Diabetes Model for Experimental Data by Using Fractional Operator, Math. Comput. Simul. 218 (2024), 133–148. https://doi.org/10.1016/j.matcom.2023.11.017.
[18] R. Caponetto, S. Graziani, I.S. Mughal, L. Patanè, F. Sapuppo, Control of Fractional Order Bergman's Glucose-Insulin Minimal Model, IFAC-PapersOnLine 58 (2024), 101–106. https://doi.org/10.1016/j.ifacol.2024.08.174.
[19] M.U. Saleem, M. Farman, A. Ahmad, E.U. Haque, M. Ahmad, A Caputo Fabrizio Fractional Order Model for Control of Glucose in Insulin Therapies for Diabetes, Ain Shams Eng. J. 11 (2020), 1309–1316. https://doi.org/10.1016/j.asej.2020.03.006.
[20] C. Uluseker, G. Simoni, L. Marchetti, M. Dauriz, A. Matone, et al., A Closed-Loop Multi-Level Model of Glucose Homeostasis, PLOS ONE 13 (2018), e0190627. https://doi.org/10.1371/journal.pone.0190627.
[21] A. Brown, E.S. Tzanakakis, Mathematical Modeling Clarifies the Paracrine Roles of Insulin and Glucagon on the Glucose-Stimulated Hormonal Secretion of Pancreatic Alpha- and Beta-Cells, Front. Endocrinol. 14 (2023), 1212749. https://doi.org/10.3389/fendo.2023.1212749.
[22] V. Subramanian, J.I. Bagger, J.J. Holst, F.K. Knop, T. Vilsbøll, A Glucose-Insulin-Glucagon Coupled Model of the Isoglycemic Intravenous Glucose Infusion Experiment, Front. Physiol. 13 (2022), 911616. https://doi.org/10.3389/fphys.2022.911616.
[23] M. Saoussane, T. Mohammed, C. Mesaoud, Adaptive Controller Based an Extended Model of Glucose-Insulin-Glucagon System for Type 1 Diabetes, Int. J. Model. Simul. 43 (2022), 282–293. https://doi.org/10.1080/02286203.2022.2068214.
[24] S. Del Prato, B. Gallwitz, J.J. Holst, J.J. Meier, The Incretin/glucagon System as a Target for Pharmacotherapy of Obesity, Obes. Rev. 23 (2021), e13372. https://doi.org/10.1111/obr.13372.
[25] S.L. Aronoff, K. Berkowitz, B. Shreiner, L. Want, Glucose Metabolism and Regulation: Beyond Insulin and Glucagon, Diabetes Spectr. 17 (2004), 183–190. https://doi.org/10.2337/diaspect.17.3.183.
[26] T. Donnor, S. Sarkar, Insulin- Pharmacology, Therapeutic Regimens and Principles of Intensive Insulin Therapy, MDText.com, Inc., South Dartmouth, 2023.
[27] M. Martcheva, An Introduction to Mathematical Epidemiology, Springer, (2010).
[28] D.G. Zill, A first Course in Differential Equations With Modeling Applications, Brooks/Cole, 2009.
[29] E. Feliu, M.L. Telek, On Generalizing Descartes' Rule of Signs to Hypersurfaces, Adv. Math. 408 (2022), 108582. https://doi.org/10.1016/j.aim.2022.108582.